JOURNAL OF MATERIALS SCIENCE **34** (1999) 4173–4179

Residual stress measurements in welded steel beam column connections by scanning acoustic microscopy

E. DRESCHER-KRASICKA
National Institute of Standards and Technology, Metals Division, Gaithersburg, MD 20899

C. P. OSTERTAG
Department of Civil & Environmental Engineering, University of California, Berkeley, CA 94720-1710
E-mail: ostertag@ce.berkeley.edu

Residual stresses which arise from thermal expansion and contraction due to welding may have contributed to the brittle fracture exhibited by welded steel beam-to-column connections during the Northridge Earthquake. These residual stresses have a strong influence on crack initiation and crack propagation in the vicinity of stress concentrations (i.e., unfused backup bar in welded steel beam-to-column connections) and account for changes in the driving force for fracture. They affect material toughness by changing the constraint condition under which fracture occurs. Currently, all methods of dealing with residual stresses are hampered by the lack of a consistent means of measuring the magnitudes and distribution of these stresses. This paper describes a new acoustic microscopy technique that allows the mapping of residual stresses in welded connections with high spatial resolution. The technique is based on the sensitivity of polarized acoustic modes to local elastic anisotropy induced by stress. The technique furthermore allows the mapping of residual stresses in a "tomographic" way by changing the frequencies of the acoustic waves. The results reveal that the magnitude of the residual stresses is influenced by the local microstructure of the steel and the weld metal. Ductile microstructures within the weld and the heat affected zone release residual stresses by yielding, whereas brittle microstructures retain residual stresses.

1. Introduction

Residual, or internal, stresses which arise from thermal expansion and contraction due to welding are a major problem in materials technology particularly in welded connections and may have contributed to the brittle fracture exhibited by welded steel beam-to-column connections during the Northridge Earthquake.

Accounting for the residual stresses is necessary for accurate assessment of the load at which brittle fracture occurs. Besides considering residual stresses as secondary stresses their effect on constraint conditions must also be considered. Constraint has been shown to produce a large effect on the fracture toughness of mild steels [1, 2]. Furthermore, the crack initiation and crack propagation of weld defects is strongly influenced by the residual stresses in the weld and the heat affected zone. An unstable fracture can develop even from small cracks that would normally be stable if residual stresses were not present. Currently, however, the development of methods to deal with residual stresses is hampered by the lack of a consistent means of measuring the magnitudes and distributions of residual stresses.

The methods available for the measurement of residual stresses may be categorized as destructive or non-destructive. The destructive methods involve the removal of part of the specimen, by cutting, drilling, as in the sectioning, slotting, hole-drilling and Sachs boring techniques [3–6]. The residual stresses are then calculated from the changes in strain that are observed as the stressed components relax as material is removed. Non-destructive methods involve X-ray diffraction, neutron diffraction and acoustic microscopy. The X-ray diffraction method is now well established [7]. In this technique strain is determined directly from measurements of atomic lattice spacing. The technique is essentially limited, however, to surface measurements as X-rays are strongly absorbed by most engineering materials. The neutron diffraction method is a relatively new technique which, in principle, is similar to the X-ray method [8, 9]. It differs in that neutrons usually penetrate several centimeters into most engineering materials and hence may be used for the non-destructive measurement of internal as well as surface stresses. However, the technique is only available at laboratories with high flux nuclear reactors or accelerator-induced neutron sources.

Attempts have been made to measure residual stresses ultrasonically by exploiting the third order

changes in elastic constants which accompany changes in residual stresses. These approaches employ measurements of the phase velocities of elastic waves [10–12]. However, these velocities vary only weakly with changes in elastic constants, so that, except for idealized laboratory setups, this approach to measure residual stresses has had only limited success. In this paper other characteristics of ultrasonic waves, which are more sensitive to changes in elastic constants than phase velocity, and which can be detected using an acoustic microscope have been employed to measure residual stresses in welded steel beam-to-column connections.

The acoustic microscopy technique we employed in measuring residual stresses in welded steel beam-to-column joints is called the Scanning Acoustic Imaging of Stress (SAIS) [13]. SAIS utilizes shear acoustic waves and leaky waves to obtain stress distributions in welded sections. Residual stresses in a material affect wave polarization and phase in an isotropic elastic medium. This gives rise to interference between waves that, in the absence of stress, would remain in phase. The resulting patterns of interference between these waves reveal the underlying patterns of stress. The acoustic microscopy technique enables us to map the residual stresses with high spatial resolution. Furthermore, it promises to provide the through thickness information to help in the "tomographic" reconstruction of internal stress fields.

2. Description of the scanning acoustic imaging of stress (SAIS) technique

Scanning Acoustic Imaging of Stress is based on the sensitivity of polarized acoustic modes to local elastic anisotropy induced by stress. In samples subjected to load the amplitude of polarized waves varies with the applied stress. The technique can be successfully applied in isotropic elastic homogeneous samples which are large in comparison with the wave length.

The acoustic images show the significant patterns caused by the differences of the amplitude values in the stressed and stress free area. The presence of internal stresses in the interior of isotropic, solid materials might be understood, in analogy to optics, as a temporary or artificial birefringence. This effect normally persists while the loads are maintained but vanishes when the stress is removed. This phenomenon is known as temporary or artificial double refraction and was first observed in optically transparent materials. The corresponding effect in acoustics is known as acoustic birefringence or trirefringence and is observed in anisotropic single crystals as well as in isotropic materials subjected to stress. In acoustic birefringence the acoustic shear wave splits into two components which travel through the stressed material with different velocities and polarizations along the principal stress axes. Since, the first observations of acoustic birefringence by Benson and Raelson in 1956 [14], the effects of stress on velocity have been extensively studied as a means of measuring the residual stress. The polarization realignment along the principal stress axes and the resulting interference of the ultrasonic waves has only recently been applied to quantitative stress evaluation. A general theory has been developed which suggests that the resultant wave amplitudes at water-solid or air-solid interfaces can be used for quantitative measurements of stress distribution and magnitude [15]. The theoretically predicted amplitudes can be compared to the intensities of the acoustic images of stress in test materials.

In acoustic microscopy, every shear mode created by mode conversion of a longitudinal refracted wave at the water-solid interface is polarized. Following the analogy to optics, one can expect that in the stressed areas the polarized shear mode will experience birefringence. The shear wave will split into two orthogonal polarized components propagating with different speeds inside the stressed volume of the normally isotropic material. The waves received from the stressed area will show a decrease or increase of intensity compared to the intensity of the arrivals from the isotropic stress free volume depending on the direction of the acting principal stresses. This occurs because the solid/water interface acts like an optical analyzer which allows only certain polarizations to return back to the receiver through the layer of water.

When the propagation direction coincides with one of the principal axes of stress the magnitude of the acoustical birefringence is proportional to the difference between secondary principal stresses. In the case of quasi-longitudinal waves the differences between the velocity in the unstressed and the stressed material is proportional to the sum of the secondary principal stresses.

Mode conversion takes place at the solid/liquid interface when two orthogonal polarized components of the shear waves convert to longitudinally polarized compressional waves, or when two orthogonal polarized shear and longitudinal components are converted into a longitudinal wave in water. The stress pattern depends upon the choice of the mode taken for the imaging and on the interference between the different arrivals with similar travel times. If one can image the plane samples using the polarized shear wave propagating perpendicular to the direction of the acting principal stresses, the intensity of the image resolves the distribution of the maximum shear stresses in the sample (the difference of the principal stresses). Imaging with longitudinal arrivals results in a stress pattern which resembles the distribution of the sums of the principal stresses. Imaging with the surface wave propagation along the surface of the sample will present the sum of the principal stresses perpendicular and parallel to the surface but perpendicular to the direction of propagation of the surface acoustic wave. The technique requires identification of the polarized pulses and their times of arrival in order to adjust the acoustic microscope time gate width and height. The technique properly used shows an instantaneous stress distribution pattern of the material tested. The limitations of the acoustic microscope technique are the requirement of flat, parallel surfaces of the sample, immersion in water or some other low viscosity liquid and a reasonably smooth surface of the sample (this becomes critical at very high frequencies).

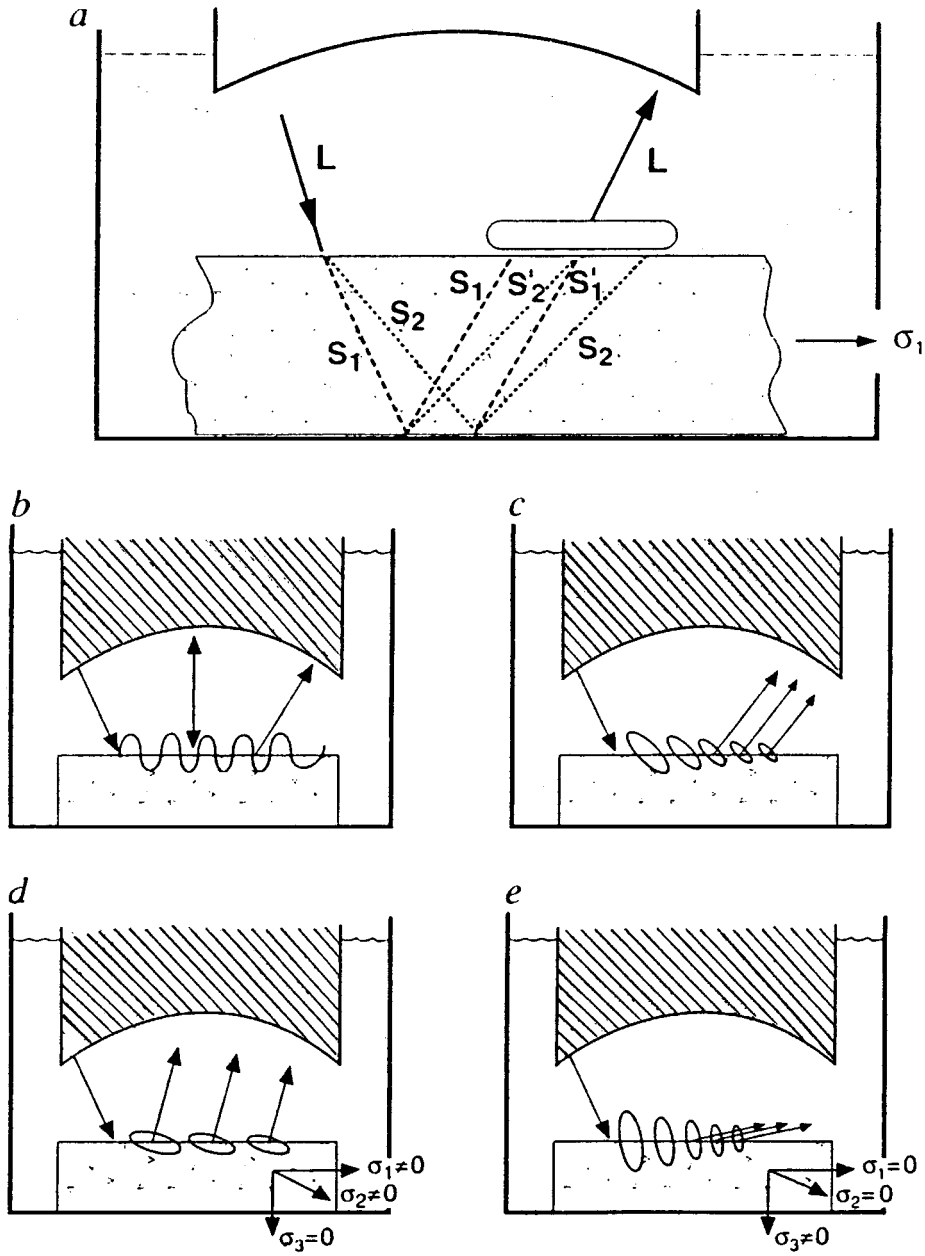

Figure 1 The SAIS technique (a) utilizing the generation of quasi-shear waves, (b–e) utilizing the generation of leaky waves.

3. Measurements of residual stresses in welded steel beam-to-column connections

Stress-induced anisotropy affects wave polarization and phase in an isotropic elastic medium. This gives rise to interference between waves that, in the absence of stress, would remain in phase. The resulting patterns of interference between these waves reveal the underlying patterns of stress. The acoustic microscopy technique enables us to map the residual stresses with high spatial resolution.

For the residual stress measurements of welded connections, we used two types of stress mapping techniques. The residual stresses were measured by the SAIS technique utilizing (1) shear acoustic waves (Fig. 1a) and (2) leaky waves (Fig. 1b–e).

(1) The SAIS in the shear acoustic mode carries information on the value and distribution of shear stresses within the weld, heat affected zone and parent metal averaged over the sample thickness. It makes use of the shear acoustic wave travelling back and forth across the steel specimen in an out-of-focus mode. In the absence of stress, the resultant shear waves would be polarized normal to their directions of propagation, in the vertical plane containing these direction shear-vertical (SV) waves. Stress, however, splits an SV wave into two "quasi-shear" waves, with their own wave speeds, and polarizations normal to each other and almost normal to their directions of propagation [15]. Each produces two reflected quasi-shear waves. The technique is illustrated in Fig. 1a. The longitudinal angular arrival through water (marked L) generates in the stressed solid two quasi-shear waves travelling with different speeds. The longitudinal reflected and refracted waves are not shown. The two shear modes S1 and S2, after reflection in the sample, create four reflected shear waves which interfere at the sample surface. The result of this interference will convert into a longitudinal wave in liquid and will be seen on the screen of the scope or

computer as an acoustic pulse. An acoustic microscope gate placed at this pulse will receive the combined amplitude of the four shear waves, which depends upon the orientation and distribution of the shear stresses averaged over the sample thickness.

Allowance for two quasi-shear waves has been made in some applications [15, 16], but the effects of multiplication of shear arrivals with each reflection have not been considered. The vertical component of motion in any one of the waves couples with the fluid on return to the front face, to produce its own longitudinal wave, transmitted back to the transducer. These longitudinal waves return with phase differences that depend on the stress in the region sampled by the shear waves. The interference pattern that results provides a map of that stress.

(2) The SAIS in the leaky mode carries information on the values and distribution of residual stresses perpendicular and parallel to the sample surface (but perpendicular to the direction of propagation of the surface acoustic wave). The microscope if used out of focus, generates "leaky waves" propagating along the solid-fluid interface, and receives the radiation produced by them. Fig. 1b–e illustrates the leaky wave created by defocused spherical transducer. Different wavelengths produce different amounts of penetration and permit control over the depth of material that is sampled. Hence, the technique can be used as a type of tomography. Different wavelengths sample different depths; very short waves will show no effect because $\sigma_3 = 0$ at the surface. The wave travels at the interface between water and sample (b). For isotropic elastic material, the image created by the surface leaky wave will be homogeneous. The characteristic asymptotic leakage angle [17] is the direction of the main energy flow. The polarization plane of the wave is perpendicular to the Poynting vector (the vector of main energy flow) and is shown (c) as an ellipse of the particle displacement. Hypothetically it can be predicted that the stresses σ_1 and σ_2 acting along the surface will cause direction-sensitive reorientation of the original polarization (d) so long as $\sigma_1 \neq \sigma_2$, and corresponding interference of signals received at the spherical lens. The postulated reorientation of the polarization plane when σ_3 has a gradient large enough for its influence to dominate, is shown in Fig. 1e. The darkest areas of the image will represent in this case the areas of highest stress.

We mapped residual stresses by the SAIS technique in a specimen cut from a welded connection that failed in a brittle manner and investigated if residual stresses are retained in the weld metal. The top surface of the sample was ground flat. The size of the specimen was 7 cm by 7 cm with a thickness of 3 cm. To map residual stresses in welded joint we used a low frequency SAM with a 1–150 MHz range. The low frequency (longer wavelength) employed for residual stress measurements ensures that the specimen appears as a homogeneous sample without "seeing" the microstructural features present within the specimen. The average wave length used for the residual stress measurements was approximately 1/5 to 1/10 of the sample thickness. The wavelength must be long enough in order not to see the microstructural features yet short enough to propagate inside the sample. We used the 2–15 MHz range. The welded steel specimens were placed in a water tank, and the acoustic scanning system was adjusted to move parallel to the surface of the sample. The shear mode and the leaky mode was excited and detected by a spherical acoustic microscope lens defocused below the surface of the sample.

Through thickness information associated with a "tomographic" reconstruction of the internal residual stress fields was obtained by using leaky waves of different frequencies. Different frequencies produce different amount of penetration and hence permit control over the depth of material that is being sampled. To complete accurate "tomographic" reconstruction of residual stress fields, the distribution of stress at the surface is needed. Surface leaky waves that propagate at the interface between the material and water contain information on the inplane surface stresses. The surface leaky wave converts into a compressional wave in water at the water-solid interface. The difference in the received wave amplitude depends locally on stresses. The specimen was probed by leaky waves using a frequency of 15 MHz. 15 MHz results in short waves which only reveal stresses within the surface layer and no stresses in the thickness direction, because at the surface $\sigma_3 = 0$. The outline of the weld is revealed as shown in Fig. 2a. There is a difference in intensities between the weld and the parent metal, indicating variations in residual stresses. The brighter weld region compared to the darker parent metal region indicates residual stresses within the surface layer of the weld. In-plane stresses are caused by constraint shrinkage of the weld in the transverse and thickness directions. Using a frequency to 2 MHz (7.5 times longer surface wave) results in a penetration depth of 2.5 mm over which the residual stresses are measured. If stresses perpendicular to the surface are dominant compared to in-plane stresses, darker regions will show up in the stress pattern. The stresses perpendicular to the surface are only dominant in the vicinity of the weld root (i.e., darker region) (Fig. 2b). In all other regions of the weld, the in-plane stresses were dominant over the depth of the material sampled. Stresses throughout the bulk of the weld is confirmed in Fig. 3, which were obtained by transmission and reflection through the thickness of the specimen of the longitudinal wave generated in out-of-focus mode. At 15 MHz, the acoustic wave penetrates the whole thickness of the specimens under investigation. Various magnitudes of residual stresses were obtained within the weld region. Dark areas correspond to the highest residual stresses, light areas indicate lower residual stresses. The weld metal in the beam-to-column connections is deposited in multiple paths, therefore, the microstructure (and hence the properties) of the early runs are completely altered by the heat from subsequent weld passes [18]. The multiple pass welding process leads to a variation in microstructures and properties ranging from brittle to ductile within the weld. The variations in residual stresses within the weld reveal a correlation between the microstructures present in the weld region and the residual stresses.

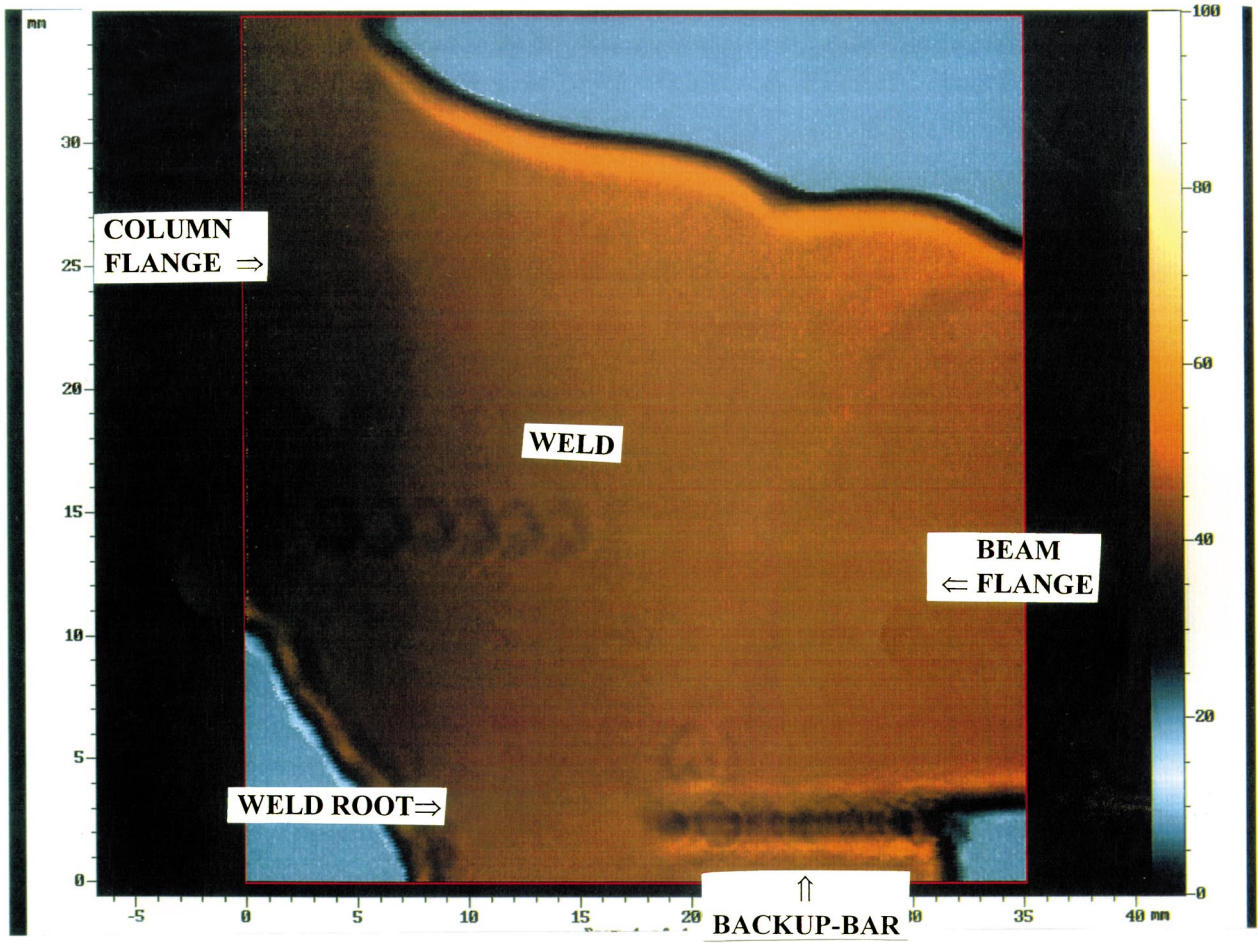

(a)

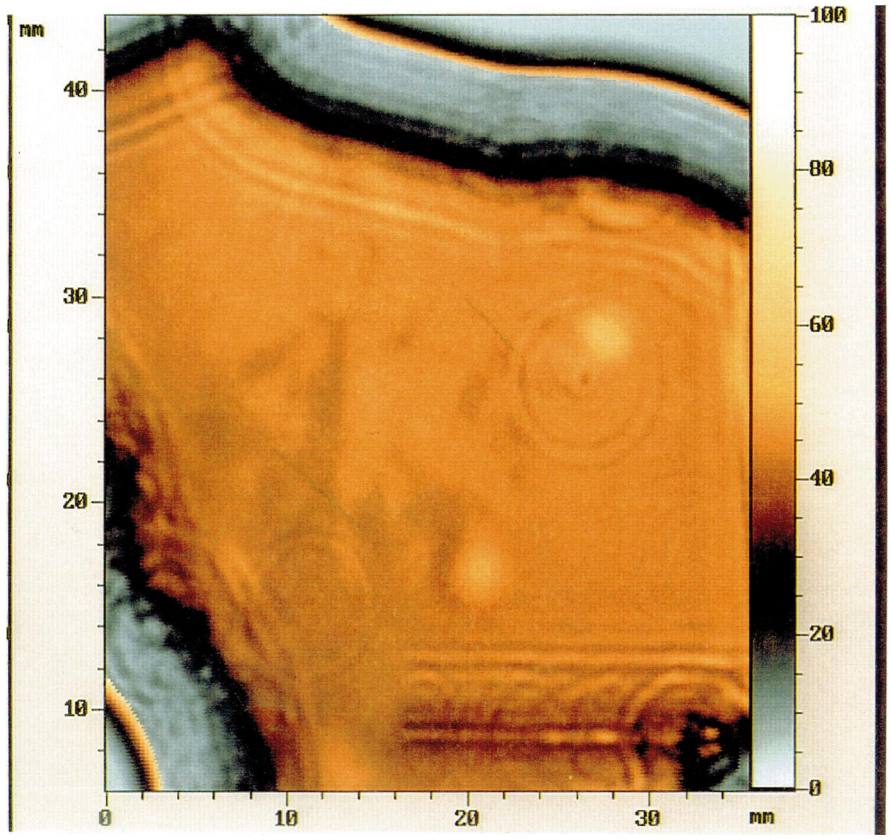

(b)

Figure 2 Stress pattern due to residual stresses in welded connection specimen utilizing leaky waves: (a) Stress pattern generated due to residual stresses that are present parallel to the surface of the specimen. The stress patterns were taken at a frequency of 15 MHz. (b) Stress patterns generated due to residual stresses that are present beneath the surface of the specimen. The stress patterns were taken at a frequency of 2.2 MHz, probing a depth of 3 mm.

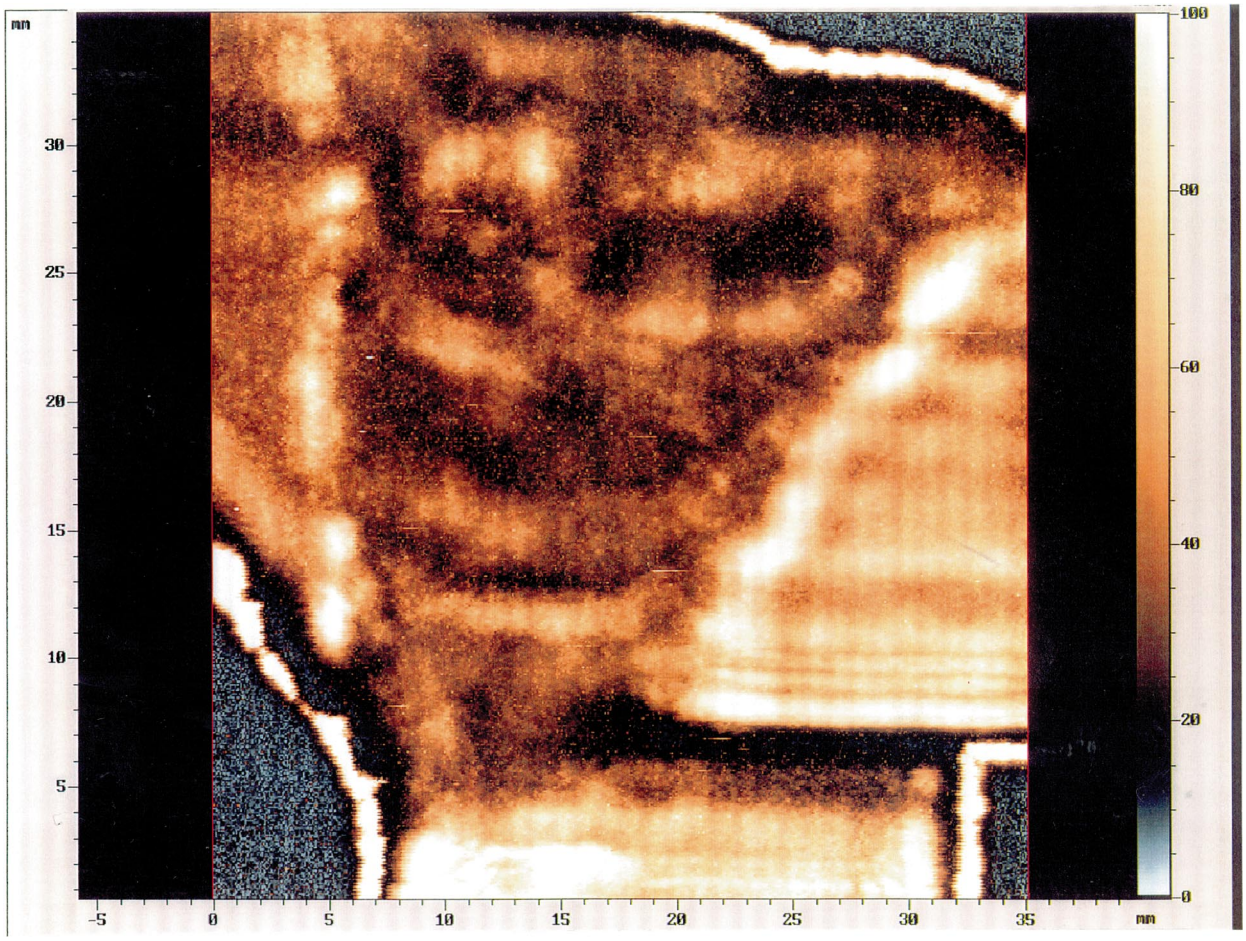

Figure 3 Stress pattern due to residual stresses in welded connection specimen. Stress pattern generated due to interference and amplitude differences of quasi-shear waves in stressed and stress free areas.

The residual stresses were lowest within the weld and the heat affected zone (HAZ) at locations where a refined, ductile microstructure formed due to the subsequent weld pass. The highest residual stresses were found at locations associated with brittle microstructures, such as in the vicinity of the weld root, last weld pass and regions within the weld. Furthermore, between and within each weld pass variations in darkness was observed, indicating different magnitudes of residual stresses. Depending on the peak temperature of the previous and successive weld passes, the brittleness of the microstructure between and within weld passes can be modified considerably. These variations in brittleness of the microstructure was confirmed by Vickers microhardness indentations [18]. Due to the high resolution of the SAIS technique, these subtle differences in brittleness of the microstructures and hence their associated residual stresses could be detected. A brittle microstructure can retain stresses, whereas a ductile microstructure relaxes the residual stresses by yielding. Regions outside the weld shown as bright areas in Fig. 3 are associated with the ductile microstructures of the HAZ. The sudden drop in residual stresses occurred over a very short distance from the fusion line towards the column parent metal. This sudden drop in residual stresses from the weld to the column face was confirmed by neutron diffraction [19].

To reduce the residual stresses in the weld the microstructure development needs to be influenced through modifications in the welding procedure. Since residual stresses induce large toughness changes ahead of a stress concentration (unfused back up bar located at the weld root is a stress concentration in welded steel beam-to-column connections), a refined ductile microstructure is essential at these locations.

4. Conclusions

We were able to measure with high spatial resolution the residual stresses in welded connections using Scanning Acoustic Imaging of Stress (SAIS). The acoustic images show significant patterns caused by the differences of the amplitude values in the stressed and stress free areas and revealed the following:

- The SAIS technique utilizing the leaky waves reveal in-plane and longitudinal stresses in the weld.
- The SAIS technique using shear acoustic waves reveals low residual stresses within the weld at locations where a refined, ductile microstructure is present. High residual stresses were found at locations associated with brittle microstructures. Since residual stresses induce large toughness changes in the vicinity of stress concentrations a refined ductile microstructure is essential at the weld root adjacent to the unfused backup bar. We recommend changes to the welding procedures to ensure that.
- The SAIS technique is a powerful technique and can be utilized as a routine check-up to obtain

information on the effect of various welding procedures applied to steel beam-to-column connections on residual stresses development in welds and heat affected zones.

References

1. W. A. SOREM, S. T. ROLFE and R. H. DODDS Jr., *Welding Research Council Bulletin* **351** (1990) 12–13.
2. T. L. PANTONIN and S. D. SHEPPARD, in W. G. Reuter, J. H. Underwood and J. C. Newman, Jr. (eds), "Fracture Mechanics," 26th Vol. ASTM STP 1256 (American Society of Testing Materials, Philadelphia, 1997).
3. G. SACHS, *Z. Metall.* **19** (1927) 352–357.
4. Y. UEDA, K. FUKUDA and M. TANIGAWA, *Trans. JWRI* **8** (1979) 249–256.
5. J. MARTHA, *Trans. ASME* **56** (1934) 249–254.
6. E. M. BEANEY and E. PROCTOR, *Strain* **10** (1974) 7–14.
7. M. R. JAMES and J. B. COHEN, *Exp. Methods Mater. Sci. Treatise on Mater. Sci. Technol*. **19A** (1980) 1–62.
8. A. J. ALLEN, M. T. HUTCHINGS and C. G. WINDSOR, *Adv. Phys.* **34** (1985) 445–473.
9. A. STACEY, H. J. MACGILLIVRAY, G. A. WEBSTER and K. R. A. ZIEBECK, *J. Strain Anal.* **20** (1985) 93–100.
10. G. S. KINO, J. B. HUNTER, G. C. JOHNSON, A. R. SELFRIDGE, D. M. BARNETT, G. HERMAN and C. R. J. STEELE, *Appl. Phys.* **50** (1979) 2607–2613.
11. S. W. MEEKS, D. P. D. HORNE, K. F. YOUNG and V. NOROTNY, *Appl. Phys. Lett.* **55** (1989) 1835–1837.
12. J. H. CANTRELL and M. QIAN, *ibid*. **57** (1990) 1870–1873.
13. E. DRESCHER-KRASICKA, *J. Acoustic Soc. Am.* **94** (1993) 453–464.
14. R. W. BENSON and V. J. RAELSON, Product. Eng. 30 (NY), "Acoustoelasticity" (1959) 56–59.
15. R. A. KLINE, L. JIANG and E. DRESCHER-KRASICKA, Rev. Prog. in QNDE, Vol. 14, edited by D. O. Thompson and D. E. Chimenti (Plenum, New York, 1995) pp. 1907–1914.
16. Y. H. PAO, W. SACHSE and H. FUKUOKA, in "Physical Acoustics," Vol. 17, edited by W. P. Mason and R. N. Thurston (Academic, New York, 1984) pp. 61–143.
17. J. A. SIMMONS, E. DRESCHER-KRASICKA and N. H. WADLEY, *J. Acoust. Soc. Am.* **92** (1992) 1061–1090.
18. C. P. OSTERTAG, *J. of Mar. Sci.*, in press.
19. C. P. OSTERTAG, E. DRESCHER-KRASICKA and H. PRASK, unpublished work.

Received 29 September
and accepted 8 December 1998